Ignition of Aviation Fuels and Surrogates in Hot Air Atmospheres – Parametric Analysis on the ASTM Injection System

SURF Final Report

Author: Hannah Ramsperger
Mentors: Joseph E. Shepherd and Charline Fouchier

Explosion Dynamics Laboratory
California Institute of Technology
Pasadena, CA
September 27, 2024

Abstract

The ignition properties of aviation fuels and surrogates are assessed in the ASTM-E659 standardized test apparatus. A small volume, 0.1-0.5 mL, of liquid fuel is injected with a syringe into hot air within a flask contained in a temperature-controlled furnace. Given that the test results strongly depend on injection characteristics, we use an automatic injection system to control the height, speed, and duration of the syringe's needle inside the hot atmosphere. We investigated how injection parameters influence ignition behavior using the temperature signals inside the flask. After conducting one hundred tests, we found that different injection parameters significantly affect the initial temperature condition and fuel volume in the flask. If the needle stays inside the flask for more than 10 seconds, approximately 150% of the initial fuel volume vaporizes. We also found that vaporization influences the temperature decrease more than the needle itself. To prove this, we visualized the injection jet with a high-speed camera in a transparent rectangular cell heated by a hot plate. This test showed that vaporized fuel enters the container even without injection, validating our hypothesis. This finding suggests that the injection in the standardized ASTM-E659 test should last less than 10 seconds to have accurate results.

Contents

1 Introduction

The self-ignition of fuels is one hazard that has to be considered in hazard analyses for process and transportation industries. Currently, aviation kerosene (Jet A) is used as fuel in all commercial airliners, but there is a search for more sustainable fuels. Before new fuels can be utilized, their autoignition temperature, among other factors, must be determined through testing. The autoignition temperature (AIT) is the minimum temperature at which a fuel ignites in a hot atmosphere without any external ignition source. The AIT of combustible liquids is measured using standardized ASTM-E659 tests [1]. While the standard is widely used in the US, interpretation of test results presents challenges and there can be significant variability as the test apparatus is not automated. The Shepherd research team, in collaboration with Boeing, is currently working on improving the protocol by enhancing our understanding of autoignition and improving test repeatability.

As earlier experiments have demonstrated, the data highly depends on experimental conditions. For instance, there is no ignition when deposits with the ignition vessel are present or when the injection height is too high. Despite efforts to make the measurements repeatable, discrepancies are observed in the AIT results. Moreover, some temperature variations remain unexplained, as complex phenomena occur inside the flask. The fact that the liquid under investigation is commodity fuel with a complex composition adds further complexity [2]. Also, since the tests are happening at comparably low temperatures, close to the AIT, the chemical process is more complex, as visible in Figure 1. The branch extending down shows the chemical process happening during ignition at low temperatures, explaining the difficulty of understanding the process inside the flask. At a temperature below 1200 K, the oxidation reaction starts with the abstraction of a hydrogen atom from the alkane molecule by oxygen. This results in alkyl (R•) and hydroperoxy (OOH•) radicals. At low temperatures under 600 K, the rapid reaction of the alkyl radicals with oxygen leads to peroxy alkyl radicals (ROO•), followed by a formation of peroxide species and small radicals. This formation enables more degenerating branching steps, resulting in more radicals. Increasing the number of radicals leads to an exponential acceleration of the reaction rate, which can cause autoignition. Since the branching steps can have different pathways, the reaction process inside the flask may depend on the fuel composition. [3]

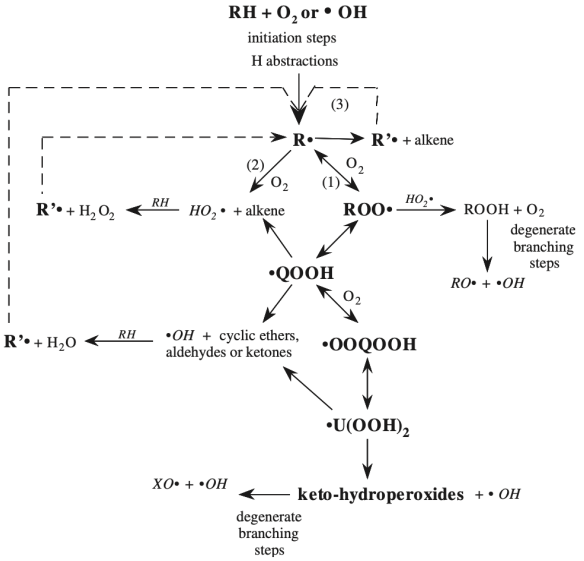

Figure 1: Simplified scheme for the primary mechanism of oxidation of alkanes taken from [3]

Recent research at Caltech suggests that measurement results strongly depend on the characteristics of fuel injection. To improve the ASTM apparatus, the Shepherd research group and his team have developed an automatic system that controls the height and speed of the fuel injection and the duration of the needle staying inside the hot atmosphere. This makes the data more repeatable and enables the investigation of how ignition behavior depends on injection [4].

The focus of the SURF project is to leverage the benefits of the new fuel injection system and investigate how various injection parameters influence ignition behavior, ultimately leading to new guidelines for a more reliable testing system. First, we ensured the repeatability of the ASTM-E659 method by conducting multiple trials to accurately determine the autoignition temperature (AIT) of hexane, used as an aviation fuel surrogate in many of my experiments. Then, we investigated the effect of the injection speed and the duration the needle stays inside the flask before and after the injection on the ignition delay time. We observed fluctuations in temperature signals during the vaporization phase, which prompted a deeper investigation into how the injection parameters influence the vaporization temperature signal. To validate the findings, we designed and constructed a new experimental setup aimed at visualizing the injection jet and the vaporization process. This setup allows to test our hypothesis that an unintentional fuel release was leading to a higher-than-expected fuel volume inside the flask. Using the background-oriented schlieren (BOS) technique, high-resolution images illustrating the vaporization process across different fuels and varying initial conditions were captured and analyzed, providing visual evidence to support our hypothesis. Finally, we investigated the injection of gaseous hexane to compare its ignition behavior with that of liquid hexane, allowing us to apply these findings to our previous parameter testing and further refine our understanding of how injection parameters influence ignition outcomes.

The remainder of the paper is organized as follows: Section 2 presents the methods and the setups used to investigate the injection, the ASTM-E659, the flow visualization, and the background-oriented schlieren. In Section 3, the results are shown and discussed. The repeatability, the AIT of hexane, the effects on the ignition delay time as well as the vaporization, the flow visualization and background-oriented schlieren results are addressed. The fourth section gives a conclusion and proposes future work.

2 Methods

2.1 ASTM-E659

2.1.1 Experimental Setup

The ASTM-E3659 apparatus, shown in Figure 2, is used to experimentally determine the AIT and was built by Conor Martin, a former Ph.D. student [5]. This apparatus consists of a 500-ml glass flask into which the tested fuel is injected inside a furnace whose temperature can be controlled. The temperature inside the flask and on the surface is measured at various locations, pictured on the schematic shown in Figure 2, using thermocouples and acquired at 75 Hz with a thermocouple acquisition module (NI 9213) from National Instruments, connected to a cDAQ-9171 CompactDAQ Chassis and controlled with a home-made LabVIEW code. Additionally, a camera and a mirror are used to observe the events inside the flask. When 0.05-0.5 mL of fuel is injected, the inside of the flask will be observed in a dark room for 10 minutes or until ignition occurs, which can be recognized by the appearance of a flame and a sudden increase in the temperature. The AIT corresponds to the lowest temperature at which an ignition is observed. This temperature is measured in the middle of the flask (refer to T4 in Figure 2). The combustion products need to be flushed by placing an aluminum cylinder inside the flask and a heat

gun above the cylinder for 30 seconds. Due to temperature fluctuations during cleaning, it is essential to wait until the temperature stabilizes before beginning the next test.

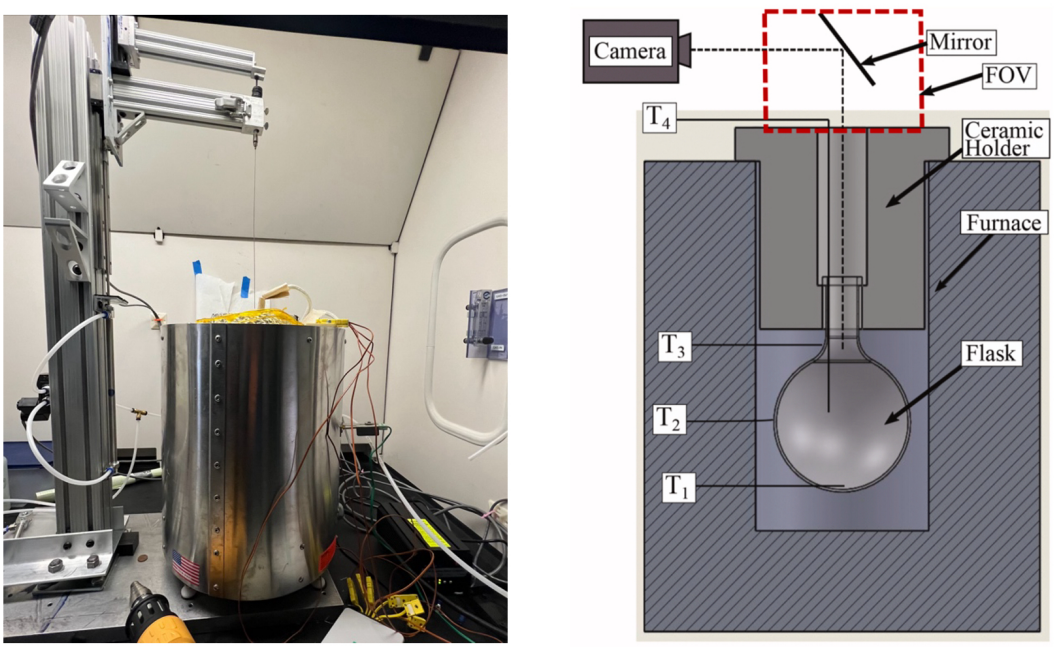

Figure 2: ASTM-E3659 test apparatus with automated injection system (left), and schematic showing of the flask with thermocouple measurement locations (right) [2]

After the ASTM testing, the following measurements are reported: the average temperature of T4 over 30 seconds before the injection, the ignition delay time, and the maximum temperature recorded inside the flask. The values are extracted from the temperature signal given by T4. Furthermore, it is noted whether a flame is observed and what ignition mode the event was, chosen from the following four modes: (I) Ignition, (II) Cool Flame, (III) Non-Luminous Cool Flame, and (IV) Rapid Reaction, described by Martin et al. [2] in Table 1. Through the measurements, diagrams can be created to illustrate the following relationships: temperature-time and temperature gradient-time. The temperature gradient is used to consistently localize the ignition delay time for each test. The ignition delay time can be identified by finding the first local maximum of the second derivative of the temperature curve.

Ignition Mode	Name	Temperature Rise	Luminosity
I	Ignition	Large	Large
II	Cool Flame	Small	Small
III	Non-Luminous Cool Flame	Large	None
IV	Rapid Reaction	Small	None
-	Non-Ignition	<15°C	None

Table 1: Classifications of ignition modes observed in ASTM-E659

During my experiments, I observed three distinct outcomes: ignition (Mode I), a non-luminous cool flame (Mode III), and no ignition. The different temperature signals for the modes are shown in Figure 3. Both definitions for Mode I and Mode III require a temperature variation. The only way to differentiate these modes is to check if there is a flame or not. Since I was exclusively testing with hexane in the ASTM-E659 setup, and the ignition delay time for hexane is known to be under 3 minutes, each test was

run for 200 seconds before the flask was flushed. The waiting time between each test was approximately 20 minutes, allowing the temperature to stabilize. The syringe was filled with 15 µL of hexane, with a margin of error of 1 µL.

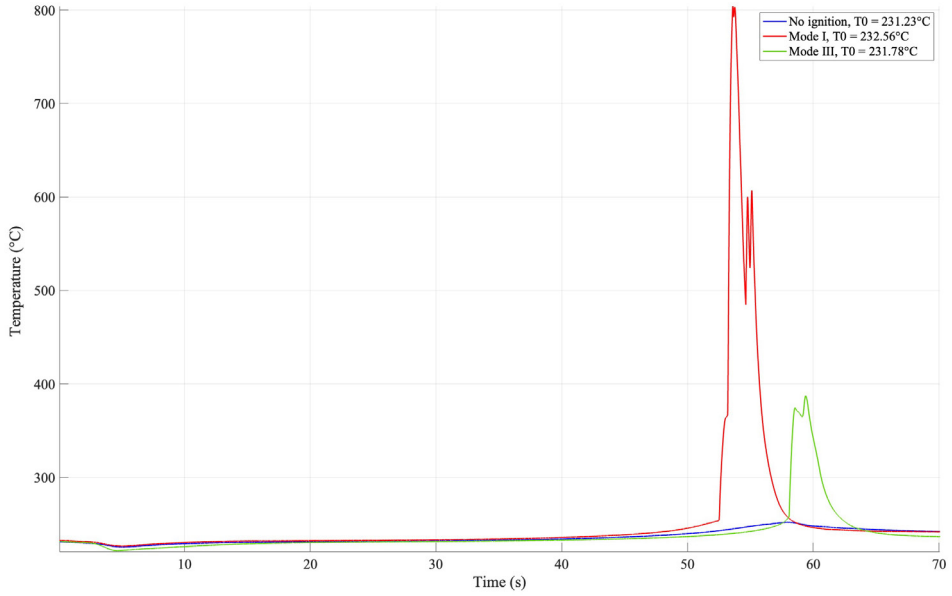

Figure 3: Temperature signals for Mode I, Mode III, and no ignition

2.1.2 Injection Parameters and Testing Configurations

The injection velocity and the duration the needle stays inside the flask before and after the injection can be controlled with the automated injection apparatus connected to the computer running the software LabVIEW. The LabVIEW code manages the whole injection as well as the recording of the temperature signal. The test timeline is summarized in Figure 4 and designed as follows. The test starts, and the initial temperature of the flask is acquired at 75 Hz for 30 seconds. The mean temperature signal from T4 is used to define the initial temperature that will be linked to the AIT. Two seconds after the initiation condition acquisition, the injection arm with the syringe is lowered inside the flask. Then, the needle waits inside the flask for a certain amount of time before injection, which can be defined by the user. I used the duration of 2 seconds, 5 seconds, and 8 seconds to investigate the influence of the duration of the needle inside the flask before the injection on the ignition behavior. Then, the fuel gets injected at a certain speed, and the temperature acquisition starts simultaneously. Depending on the analysis, the needle is removed from the flask 3, 6, 9, 15, 21, or 40 seconds after the start of the injection. Part of this duration is the injection, whose required time depends on the injection speed. The motor controls the injection speed, with values expressed as a percentage of the motor's maximum velocity. By default, the injection speed is set to 15%, resulting in an injection time of approximately 1.2 seconds. The default setting is that the needle is 2 seconds inside the flask before the injection and removed 3 seconds after the start of the injection, with a speed of 15% of the maximum velocity. Afterwards, the injection arm rises and turns away from the flask within 2 seconds. Finally, one must wait until the acquisition time of a maximum of 200 seconds has expired and the test has ended.

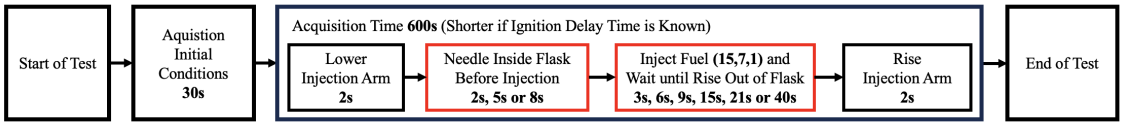

Figure 4: Timeline of the injection systems indicating which parameters have been investigated (red)

For the testing, only one parameter at the time has been changed except when the speed has changed because then the injection took longer, which is why the time the needle stays inside the flask during and after the injection must be extended. I have defined the following configurations characterized by the injection parameters:

Configuration	Injection Speed (%)	Before Injection (s)	After Injection (s)
1	15	2	3
2	15	2	8
3	7	2	8
4	1	2	8
5	15	5	3
6	15	8	3
7	15	2	6
8	15	2	9
9	15	2	15
10	15	2	21
11	15	2	40

Table 2: Injection Parameter Definition of Configurations for ASTM-E659 Testing

2.2 Flow Visualization and Background-Oriented Schlieren

The setup for the flow visualization and background-oriented Schlieren method consists of a transparent rectangular cell on a hot plate and is shown in Figure 5. Inside the cell is another smaller cell with a second glass plate elevated with ceramic to imitate the ASTM test, where the flask does not directly touch the hot ground. However, the second floor was removed after Test 19 as the droplets bounced under the glass plate, causing ignition problems. A hole is placed on the top of the cell to inject the fuel using the syringe. The cell was surrounded with wool glass and aluminum foil for thermal insulation, as shown in Figure 6.

Two Phantom high-speed cameras were placed in front of the cell to record the jet using two different techniques. Due to the small space, one technique has to be recorded via a mirror. An LED lamp was placed behind each of the two backgrounds, and diffusive panels were used to have homogeneous light. A speckled background was attached to one of the diffusive panels to apply the background-oriented Schlieren (BOS) technique. Examples of unprocessed experimental images obtained with flow visualization (left image) and BOS (right image) are given in Figure 7. The high-speed cameras were controlled with the PCC software, where the frequency of frames per second and the exposure time can be selected. While one person injects the fuel manually, the other person triggers both cameras simultaneously using a signal generator. The temperature inside the cell was measured with four thermocouples whose approximate positions are indicated in the figure. The temperature T3 was measured in air at approximately the same point as T4 in the ASTM testing flask.

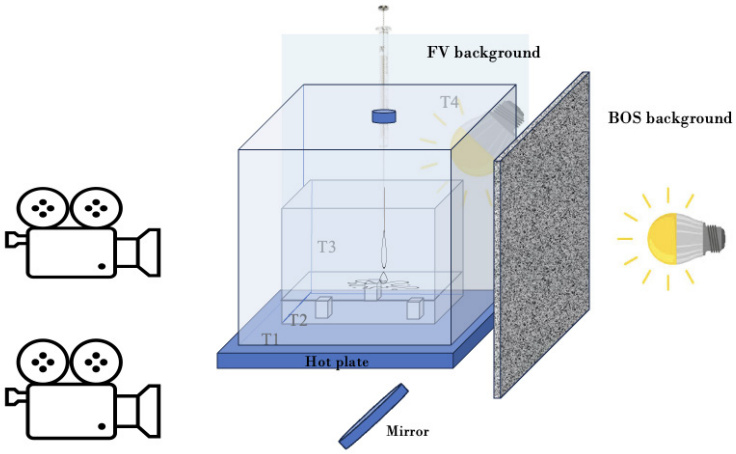

Figure 5: Diagram of cell setup for flow visualization and BOS

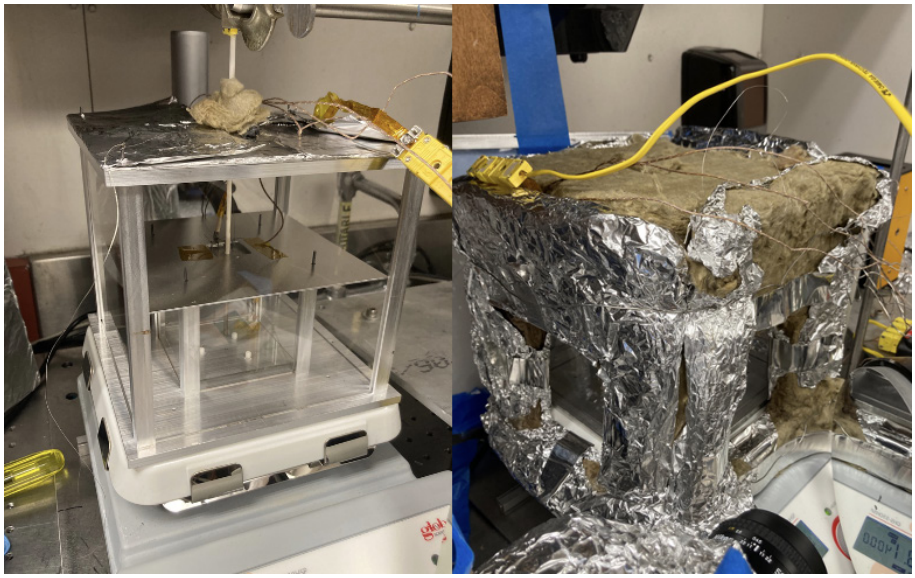

Figure 6: Picture of the cell setup with (right) and without (left) thermal insulation

Figure 7: Experimental images of the flow visualization (left) and the BOS (right)

The droplet injection and vaporization are captured with the flow visualization technique. The intense LED light shines through the diffuse panel, which serves as a background to see the injection clearly.

The fuel vaporization and vapor dispersion are investigated using the BOS technique. The density change inside the cell due to hexane vaporization leads to local modification of the light path, then local displacements of the background dots observed on the camera image. By cross-correlating the images one with the other using PIVlab, a digital particle image velocimetry tool for MATLAB, the displacements can be processed, and the strong displacement vectors can highlight the vapor propagation.

We tested at a temperature at T3 (air temperature inside the cell) of 190°C and 290°C with a fuel volume of 100 µL. The temperatures were chosen based on the Leidenfrost temperature of hexane, 130-135°C [6], and the AIT of hexane, 230-235°C. The temperature of the surface is higher than the Leidenfrost temperature of hexane. The Leidenfrost effect is a physical phenomenon that occurs when the surface temperature is much higher than the boiling temperature of the liquid, causing the formation of an insulating vapor layer around the droplets, which slows down the evaporation drastically.

The injection speed is different for every test because of the manual injection. The time the needle is inside the hot atmosphere before the injection varies between 0, 30, and 60 seconds. The needle was removed right after the injection. For the comparison of the vaporization of different fuels, we used hexane, Jet A POSF-4658 [2], Synthetic Paraffinic Kerosene (SPK) [4] and 10% TMB, which is a solution of 90% n-nonane and 10% 1,2,4-trimethylbenzene.

For the high-speed camera settings, an exposure time of 10 µs was chosen. A frequency of 500 fps was selected to capture the entire vaporization process, while 1500 fps was chosen for capturing a short, detailed sequence of the injection.

3 Results and Discussion

3.1 Repeatability and Determination of AIT

For test repeatability, the initial conditions and the injection have to be as similar as possible. Referring to the timeline of a test (Figure 4), the mean temperature measured within 30 seconds of the acquisition of the initial conditions must be close to each other, and the injection parameters must be the same. A comparison of the temperature signal of two tests at similar experimental conditions is given in Figure 8. The description of the tests is given in Table 3. The initial part of the curve (before 20 seconds), where the temperature drops due to the fuel vaporization inside the flask, can be used to assess the repeatability of the injection. The subsequent temperature variation is due to the exothermic reaction of the fuel subjected to the hot atmosphere of the flask. The similarity of the curves under similar conditions suggests a relatively good repeatability of the injection, allowing for the experiments to be compared. This repeatability was observed for all tests with the same configuration and initial temperature.

Each temperature signal figure in this report gives in the legend the initial temperature of the studied test, named T0, calculated from the mean of the 30-second measurement before each test. T0 is given with two digits after the comma. This does not represent the measurement accuracy, as the accuracy of the thermocouple is +/- 2°C, and the temperature inside the flask is not perfectly homogeneous and can vary by several degrees [4]. The value is, however, useful for test comparison purposes.

In Figure 9, it is observed that a temperature difference of less than 1°C (233.38°C versus 232.59°C) already has a visible impact on the ignition delay time. The ignition characteristics are listed in Table 4. However, the injection is reproducible with the automated apparatus, as the temperature variation before 20 seconds is similar for all tests. By

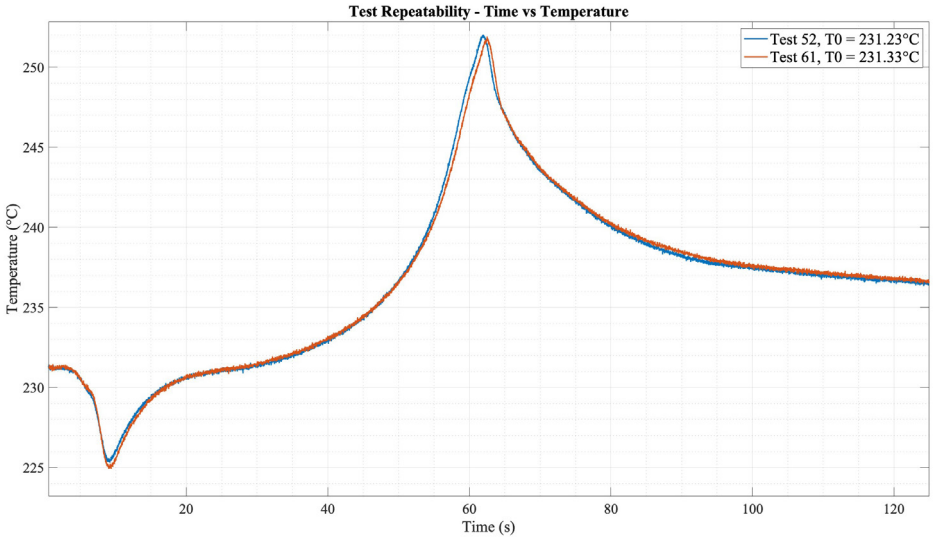

Figure 8: Plot showing temperature signal of T4 during the test with configuration 1 to prove test repeatability

Test	Initial Temperature	Ignition Delay Time	Maximum Temperature
52	231.23°C	no ignition	252.0°C
61	231.33°C	no ignition	251.9°C

Table 3: Ignition characteristics of Test 52 and 61

proving the reliability of the apparatus, the investigation of the injection parameters can be targeted and reliable. Since the curve of Test 54 has a double peak and the other does not, one can also see that it is difficult to identify what is happening in the flask during the ignition and that each test shows a different ignition behavior inside the flask. Figures 8 and 9 are examples of graphical comparisons, which have been done for all the tests and configurations and have also been used to compare the influence of each parameter.

Some tests have been conducted close to the AIT to investigate the effect of the injection on the AIT. Since the AIT values for hexane provided by the literature vary, I measured it myself. The ignition of hexane was measured to happen between T0=231.2°C and 232.3°C with configuration 1, results are shown in Figure 10 and Table 4. In our case, Mode III ignition (no flame) is considered as ignition, following the practice of Fouchier and Shepherd. [4]. The link between AIT and the T0 is not straightforward and requires more tests at various fuel volumes, supported by a statistical analysis [4]. As the accurate estimation of the AIT was not the goal of this project the value given by T0 is used.

Test	Initial Temperature (T0)	Ignition Delay Time	Maximum Temperature
51	229.4°C	no ignition	244.0°C
52	231.2°C	no ignition	252.0°C
53	233.3°C	47.6 s	806.2°C
54	232.6°C	52.5 s	804.1°C

Table 4: Ignition characteristics of Tests 51, 52, 53 and 54

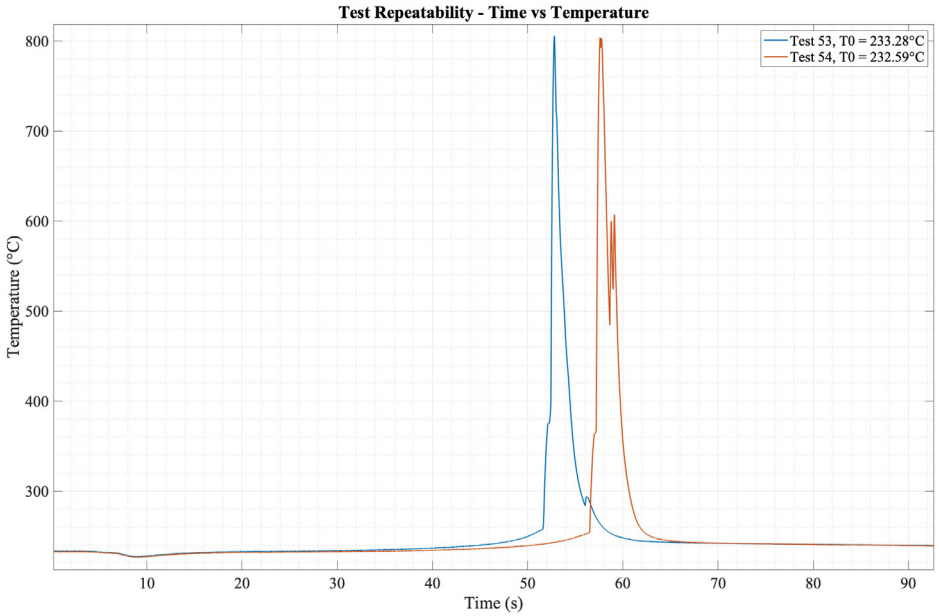

Figure 9: Plot of temperature signal of T4 with configuration 1 to show the importance of initial temperature and variety of ignition behavior inside the flask

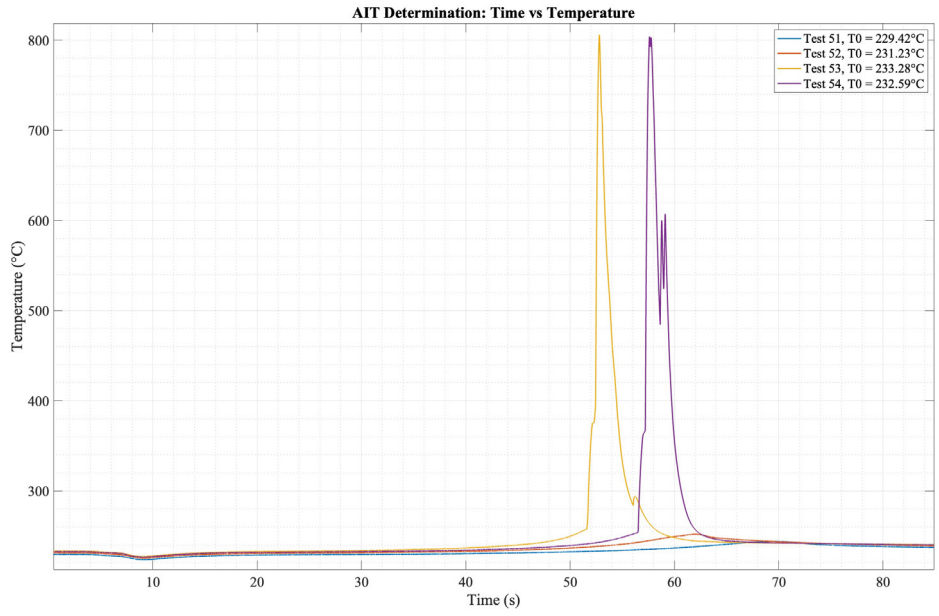

Figure 10: Plot of temperature signal of T4 with configuration 1 used to determine T0 values bracketing the AIT condition

3.2 Effect of Needle

Each T4 temperature signal of an ASTM-E659 test has a similar time history: it starts with a stable temperature before the injection, and after the injection, the temperature decreases. After 10 - 15 s, the injection transient is over, and the temperature increases to the initial value again. Then, the ignition process starts, beginning with a slow temperature rise and ending with a sharp increase in temperature. The time between injection and

the sharp temperature rise is the ignition delay time. After the ignition, the temperature drops again.

Two possible factors could cause the first temperature drop: the cold needle entering the flask, and the vaporization of the fuel since the change from liquid to vapor takes thermal energy from the surroundings. To find out which of these components has the bigger impact, an ASTM test without fuel was conducted, and the temperature signal was plotted a bit before the needle entered the flask. The acquisition was started 4 seconds before the injection to investigate the effect of the needle entering the flask.

In Figure 11, it can be seen that the temperature conditions are stable before the injection, and when the needle goes inside, there is a slight temperature decrease. Moreover, the slope of both curves is the same between 0 and 4 seconds since this is the initial condition acquisition and between 4 and 6 seconds, where the needle enters the flask. Thus, the slope between 4 and 6 seconds is the effect of the cold needle entering the flask. Afterward, there is no visible correlation between the signal, meaning that the big decrease is due to the injection of the fuel and its vaporization.

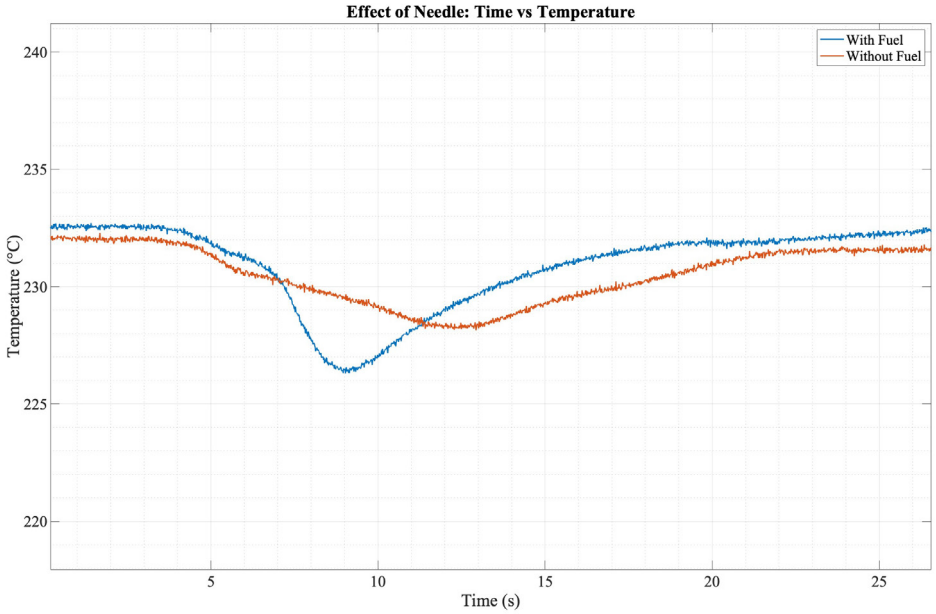

Figure 11: Comparison of T4 temperature signal with and without fuel to investigate the effect of the needle on the initial temperature decrease

3.3 Effect on Ignition Delay Time and Vaporization

To investigate the impact of the injection parameters on the ignition delay time, preliminary tests have been conducted at a temperature range between 247°C and 250°C of T4. After the first results, a selection of tests was done at a temperature around the AIT, 231-233°C, to further investigate the vaporization, as ignition is more sensitive to experimental conditions around this value. The ignition delay time can be extracted from the temperature signal recorded by T4. As shown in Figure 12, the ignition time is located at the start of the sharp increase leading to the peak. The temperature signal begins recording when the injection starts, and after a few seconds, a decrease in temperature can be observed. Following this decrease, the temperature stabilizes until ignition occurs, resulting in a large peak. After ignition, the temperature stabilizes once more. During preliminary tests, we observed variations in the first temperature decrease depending on parameter changes, so we focused our analysis on this temperature drop.

3.3.1 Injection Speed

Three injection speeds have been compared (1%, 7%, and 15%). The computation of the injection speeds is explained in Section 2.1.2. It is visible in Figure 12 that the temperature signal is only different during the first 15 s before the ignition. Since the ignition delay time close to the AIT is longer than 15 s and the ignition delay time for different injection speeds shows a variation of less than 0.3 s, there is no visible effect of the injection speed on the ignition delay time or ignition behavior. However, the temperature signal during the vaporization does depend on the injection speed. The slower the speed, the smaller the temperature drop is. During the test with a speed of 1%, an unsteady temperature signal during the vaporization was recorded. It also takes a longer time to inject the fuel at 1%. This can be an issue when a larger volume of fuel needs to be tested. Thus, it is advised to inject the fuel at a faster speed.

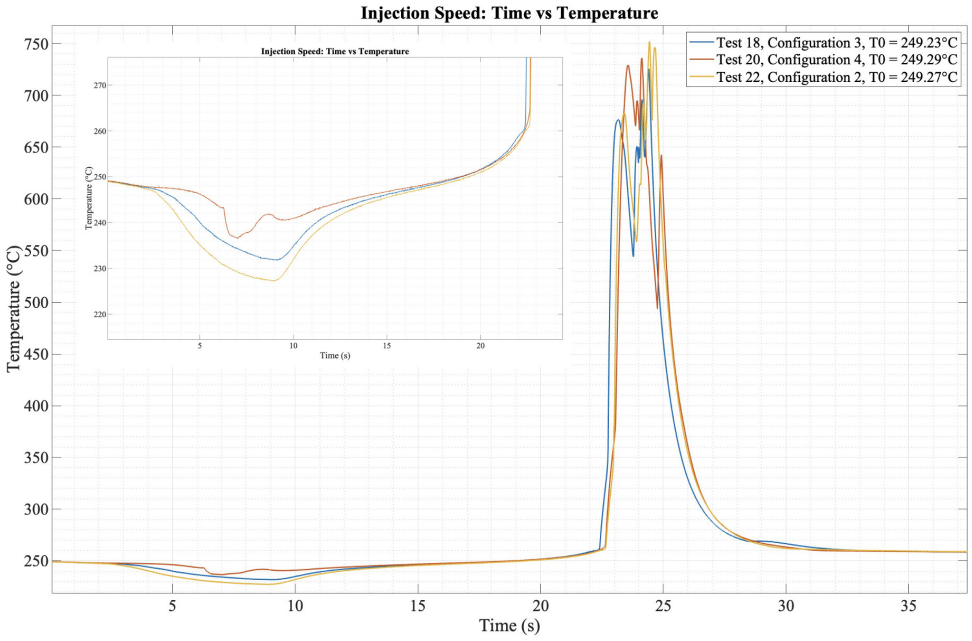

Figure 12: Temperature signal of tests conducted at different injection speeds

Test	Initial Temperature	Ignition Delay Time	Max Temperature	Injection Speed
18	249.2°C	22.4 s	725.9°C	7%
20	249.3°C	22.6 s	736.2°C	1%
22	249.3°C	22.7 s	752.1°C	15%

Table 5: Ignition characteristics of Tests 18, 20 and 22

3.3.2 Needle Inside the Flask Before the Injection

As shown in Figure 13, there is a visible shift of the ignition delay time depending on the time the needle is inside the flask before the injection. The longer the needle is inside before the injection, the sooner the ignition happens. However, the difference between Test 24, where the needle is inside for 2 seconds, and Test 31, where the needle is inside for 8 seconds, is less than 4 seconds, and the initial temperature is also half a degree higher for the test with an earlier ignition delay time. To see if testing closer to the AIT has a bigger impact, configurations 1 and 6 have been tested at 232°C (Table 6). Indeed, there is a bigger shift in the ignition delay time, showing that if the needle stays inside longer, the ignition happens faster.

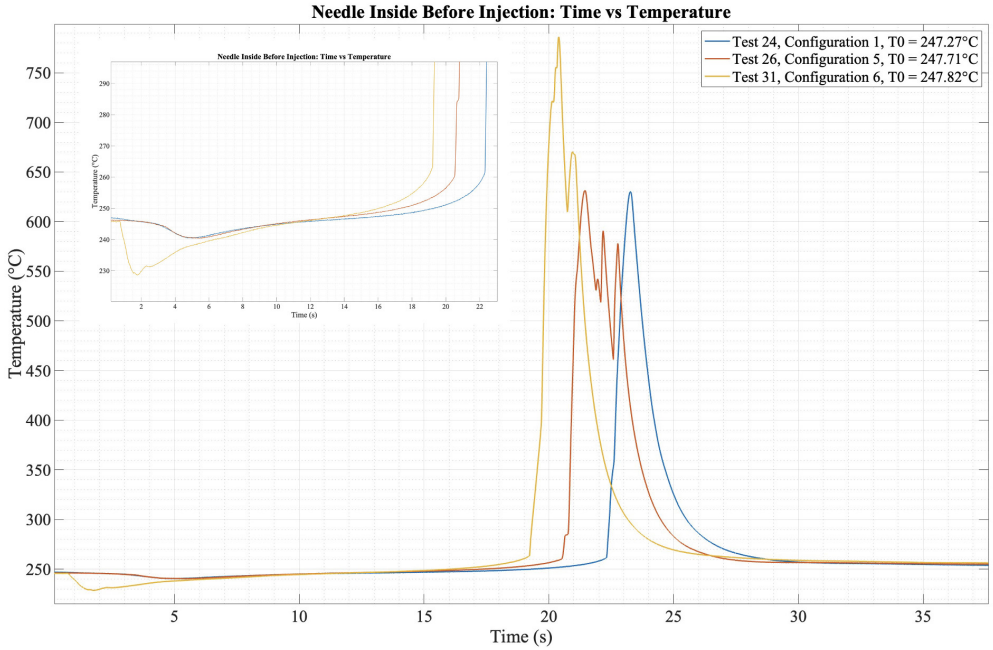

Figure 13: Temperature signal of testing series with different durations of the needle staying inside the flask before the injection

Test	T0	Ignition Delay Time	Config.	Needle Before Injec.
24	247.3°C	22.3 s	1	2 s
26	247.7°C	20.5 s	5	5 s
31	247.8°C	19.2 s	6	8 s
62	232.3°C	52.2 s	1	2 s
81	232.4°C	66.4 s	6	8 s

Table 6: Ignition characteristics of Tests 24, 26, 31, 62 and 81

The duration of the needle stays inside the flask before the injection also affects the vaporization temperature signal. For 2 and 5 seconds, it appears to be the same; however, for 8 seconds, the temperature decrease happens sooner and more extreme. The longer the needle is inside, the hotter the fuel gets inside the needle. This leads to vaporization right at the exit of the needle as opposed to configurations 1 (2 seconds) and 5 (5 seconds), where the injected fuel first hits the ground of the flask, and the droplets bounce before vaporizing. Thus, for configuration 6 (8 seconds), the vaporization happens closer to the thermocouple T4, which is why the temperature drop is recorded earlier, and the cooling signal is larger. This accelerated vaporization starts when the needle is inside the flask for 8 seconds or more.

3.3.3 Needle Inside the Flask After the Injection

As shown in Figure 15, the duration the needle stays inside the flask after the test affects the ignition delay time. In Table 7, it can be seen that with increasing duration, the ignition delay time increases. If the needle is inside the flask for 37 seconds or more, the ignition delay time is 20 seconds longer. The effect of changing the duration the needle stays inside after the injection is shown in Figure 16. The time at which the needle is removed from the flask is highlighted by a diamond symbol for each test. However, looking at the time of the removal of the needle and the temperature increase after the vaporization, no correlation can be found.

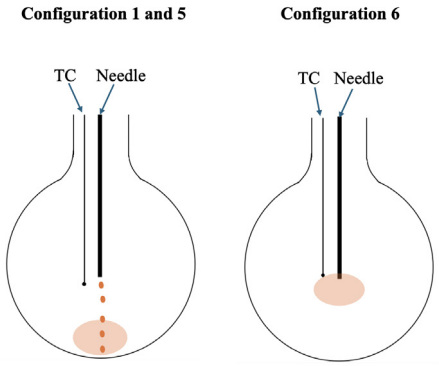

Figure 14: Schematic explanation for different vaporization temperature signals with different durations of the needle staying inside the flask before the injection (TC = Thermocouple)

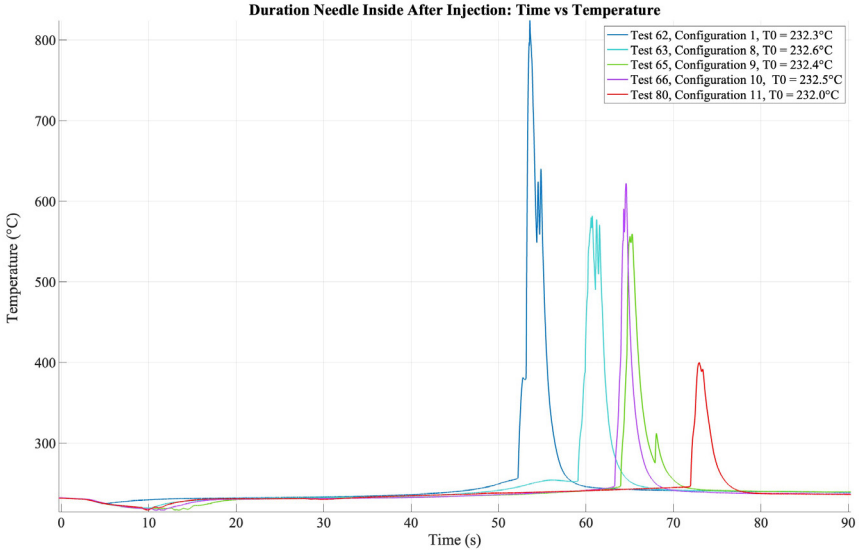

Figure 15: Temperature signal for tests with a different duration of the needle staying inside the flask after the injection

Test	Initial Temperature	Ignition Delay Time	Confi.	Needle After Injec.
62	232.3°C	52.2 s	1	3 s
63	232.6°C	59.1 s	8	9 s
65	232.4°C	64.0 s	9	15 s
66	232.5°C	67.3 s	10	21 s
80	232.0°C	72.0 s	11	40 s

Table 7: Ignition characteristics of Tests 62, 63, 65, 66 and 80

Nevertheless, the duration of the needle staying inside the flask after the injection has an impact on the vaporization, as every temperature signal is different. An important observation is that if the needle is inside longer than 9 seconds, a strange noise is heard and a strong temperature variation occurs. This happened because the needle was getting too hot, and the fuel inside was vaporizing, leading to an unintentional second injection, causing an increase in fuel concentration inside the flask. This hypothesis was verified using the square cell with optical techniques (Chapter 2.2).

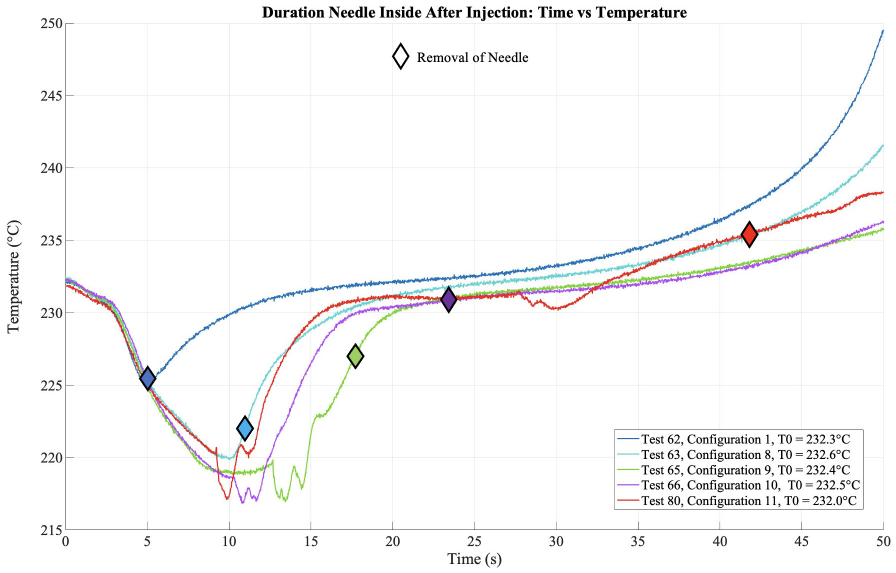

Figure 16: Time signal for the ASTM tests investigating the effect of the duration of the needle staying inside the flask after the injection. The time at which the needle is removed from the flask is highlighted by a diamond symbol for each test.

3.3.4 Arrhenius Plot and Activation Energy

The Arrhenius plot can be used to illustrate the effects of the injection on the ignition delay time of all configurations. The ignition delay time can be modeled using an Arrhenius expression for many fuels

$$\tau_i = ae^{Ea/(RT)} \tag{1}$$

where a is a constant value, Ea the activation energy of the studied fuel in $\mathrm{J \cdot mol^{-1}}$, R the gas constant in $\mathrm{J \cdot K^{-1} \cdot mol^{-1}}$, T the temperature in Kelvin, and τ_i the ignition delay time in seconds.

By taking the logarithmic value of the ignition time and the inverse of the initial temperature, we obtain an Arrhenius plot. If the plotted relationship can be approximated as linear, the activation energy can be experimentally measured by estimating the slope b of the linear fit ($b = Ea/R$) as explained by Fouchier et al.[4] The Arrhenius plot obtained with all the experimental data is given in Figure 17. It shows that the configurations have some impact on the ignition delay time because the values are scattered around the linear fit. However, the most significant effect is the initial temperature since the clusters formed by different configurations do not show apparent trends.

For the line of best fit with all the configurations $a = 6.07 \cdot 10^{-11}$ s and $b = 1.39 \cdot 10^4$ $\mathrm{K^{-1}}$. The activation energy can be calculated by multiplying the constant b with the gas constant $R = 8.31446$ $\mathrm{J \cdot K^{-1} \cdot mol^{-1}}$. Combining all configurations, the activation energy for 0.1 mL of hexane is $Ea_{all} = 115$ $\mathrm{kJ \cdot mol^{-1}}$. Enough tests at different temperatures have been conducted with configuration 1 alone so that an estimation with a linear fit is possible. The activation energy of hexane with just configuration 1 is $Ea_1 = 106$ $\mathrm{kJ \cdot mol^{-1}}$. This is consistent with the initial step of low-temperature oxidation, the conversion of hexane to hydroperoxy-ketones with an effective activation energy between 100 and 110 $\mathrm{kJ \cdot mol^{-1}}$. [7]

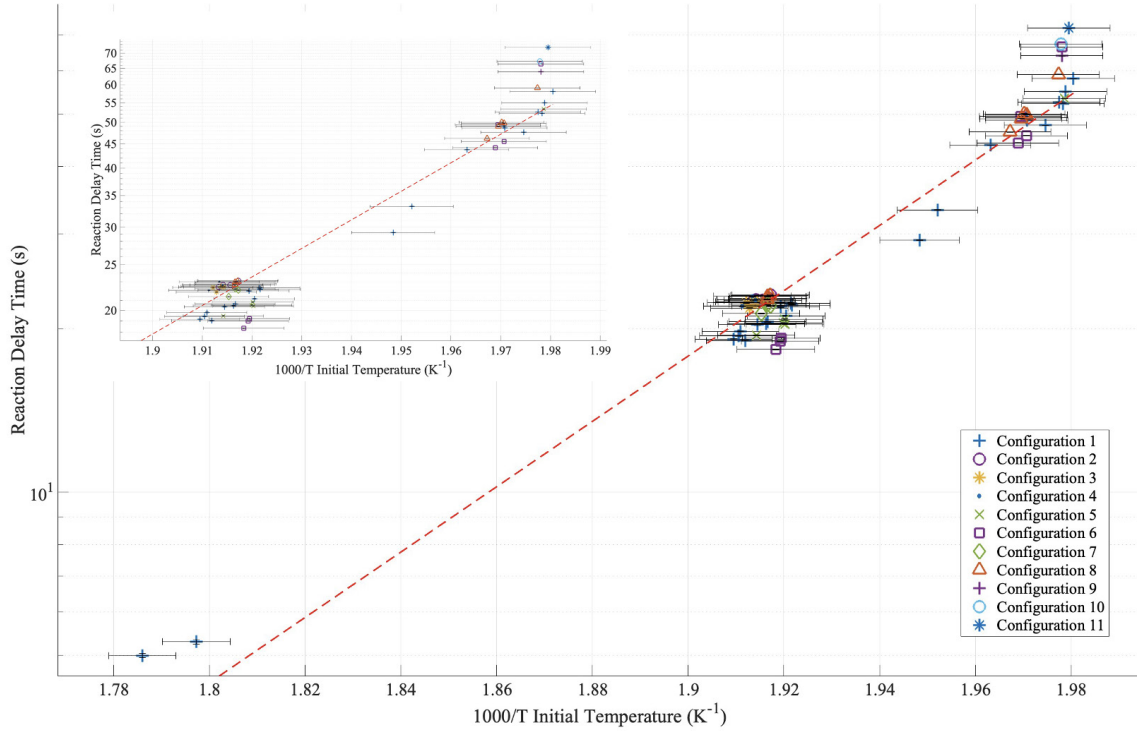

Figure 17: Arrhenius plot with all configurations to show the influence on the reaction delay time and the line of best fit to estimate the activation energy. The inset plot shows the initial temperature range closer to the AIT (T0).

3.4 Thermal Energy for Vaporization of Hexane

During the initial temperature drop, the injected fuel changes its aggregate state from liquid to gas due to the air temperature above hexane's boiling point. This change absorbs thermal energy from the air and causes the temperature measured by T4 to drop. To calculate how much thermal energy from the air is required to vaporize the fuel, an idealized energy balance is used

$$m_{fuel}\Delta H_{hexane} = m_g c_p \Delta T \tag{2}$$

where m_{fuel} is the mass of the injected fuel, which can be calculated using the density of liquid hexane, ρ_{hexane}, [8] and its volume, ΔH_{hexane} is the molar enthalpy of vaporization of hexane [9], m_g is the mass of gas providing the thermal energy, c_p is the specific heat capacity of air [10], and ΔT is the temperature drop inside the flask. The following values are used to calculate m_g and the volume of the affected air V_g:

ρ_{hexane}	660 kg $\cdot$ m^{-3}
V_{hexane}	0.1 mL kg $\cdot$ m^{-3}
M_{hexane}	86.18 g $\cdot$ mol^{-1}
ΔH_{hexane}	28.9 kJ $\cdot$ mol^{-1}
c_p	1.01 J $\cdot$ g^{-1} $\cdot$ mol^{-1}
ΔT	10 K
ρ_{air}	0.67 kg $\cdot$ m^{-3}

(a)

m_{fuel}	0.066 g
m_g	2.2 g
V_g	3.3 L

(b)

Table 8: (a) Properties and measured values, and (b) calculated values used to investigate the thermal energy required for vaporizing hexane

This estimate implies that 3.3 L of air is cooled down by vaporizing 0.1 mL fuel with a 10 K temperature difference (average value observed during our tests). The estimated adiabatic temperature decrease would be 66 K for 0.1 mL vaporized in a 500 mL flask filled with air. This value is much higher than the one measured during our tests and shows that the cooling is not adiabatic and that heat transfer from the flask is a significant factor.

3.5 Flow Visualization

Visualization was used to characterize the flow from the needle during the injection and to quantify the vaporization. Depending on the injection parameters, the fuel enters the cell as big droplets, a jet, and small droplets, or a multiphase vapor/liquid jet. The droplet behavior and vaporization process differ for each type of injection process. In Figure 18, the result of a slow injection speed is shown. A big droplet reaches the hot surface and then breaks into smaller droplets, which bounce around due to the Leidenfrost effect. This phenomenon decreases the evaporation rate drastically. Figure 19 illustrates the injection and droplet bouncing as if it would be in the ASTM test with configuration 1, the configuration set by default. Smaller droplets are followed by a jet hitting the ground, splashing, and very thin droplets form and bounce before they vaporize. If the needle stays inside the flask for 30 s or more, the fuel comes out as a multiphase jet with gaseous hexane and some liquid droplets, as shown in Figure 20. As soon as the fuel reaches the hot surface, it vaporizes. The same phenomenon occurs when an accidental fuel release happens during the ASTM tests where the needle is more than 6 seconds inside the hot atmosphere.

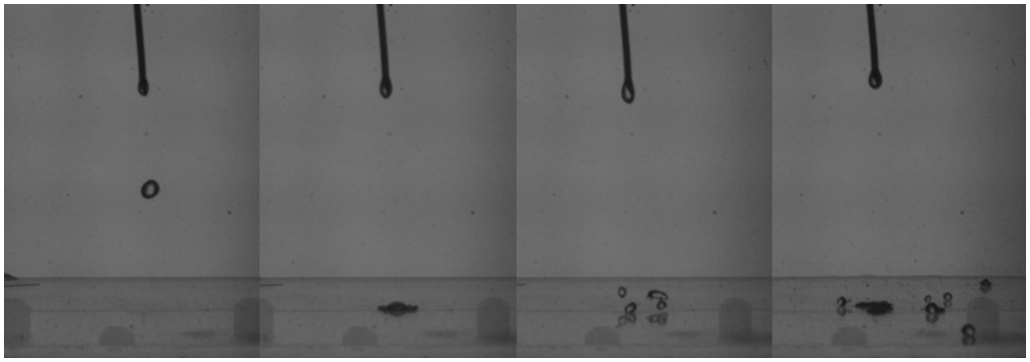

Figure 18: Big droplet injection

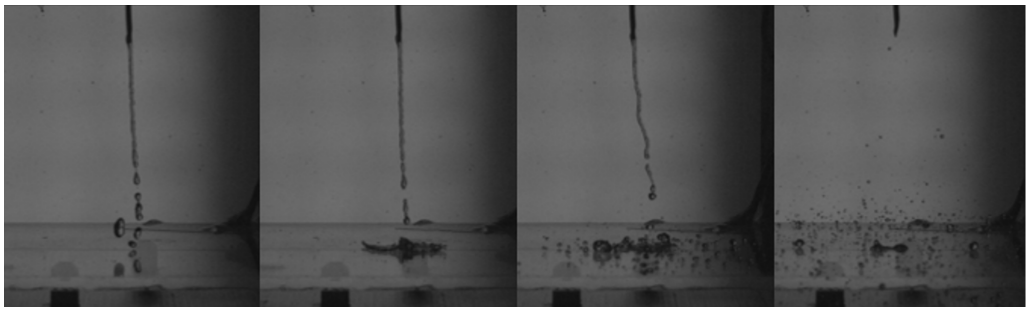

Figure 19: Usual jet injection

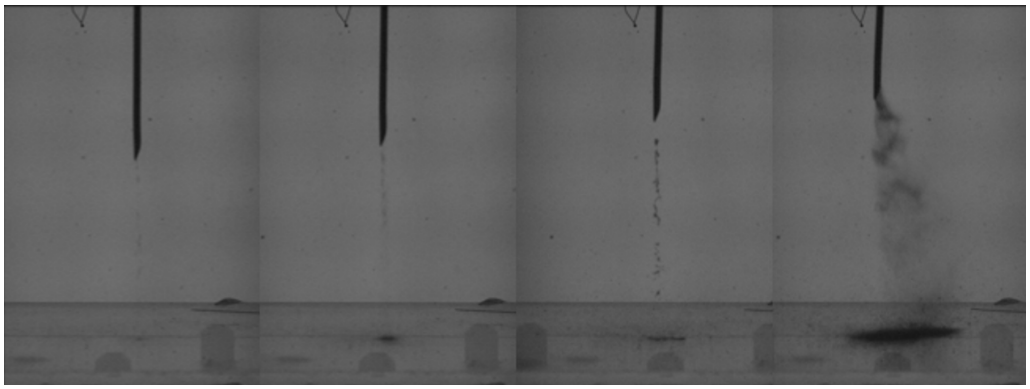

Figure 20: Multiphase vapor jet injection

By comparing two consecutive images, the jet and droplet velocity and diameter can be calculated with the results shown in Table 9. The table shows that the multiphase injection is more than six times faster than one big droplet and more than four times faster than the usual injection jet. The droplet diameter of a big droplet injection, as shown on the left in Figure 18, was extracted as a measurement reference to validate the processed displacement values.

Droplet Diameter	1.3 mm
Droplet Velocity	260 $\text{mm} \cdot \text{s}^{-1}$
Usual Jet Velocity	430 $\text{mm} \cdot \text{s}^{-1}$
Multiphase Jet Velocity	1800 $\text{mm} \cdot \text{s}^{-1}$

Table 9: Droplet diameter and needle output velocities

An estimation of the vaporization time was made by taking the time of injection until the last droplet was vaporized. Since the injection was made manually, the times just serve as an idea of the duration and cannot be reliably compared. However, it can be seen that the ignition happens before all of the fuel is vaporized. This observation is very interesting, as the fuel quantity involved in the ASTM ignition process might be lower than the injected amount.

	Hexane	Jet A	SPK	10% TMB
Injection	0.3 s	0.1 s	0.2 s	0.15 s
Ignition	1.5 s	0.9 s	0.8 s	0.75 s
Evaporation Time	$> t_{ignition}$	$> t_{ignition}$	$> t_{ignition}$	$> t_{ignition}$

Table 10: Duration of injection, time of the start of ignition, and duration of fuel vaporization at 290°C at T3 with an instantaneous injection for hexane, Jet A, SPK, and 10% TMB

For hexane, the vaporization time was determined at a temperature of 190°C and 290°C, and the time the needle was inside the cell before injection varied between 0 s, 30 s, and 60 s. With an instantaneous injection, the vaporization time was more than 4 s at 190°C and 4 s at 290°C. However, when the needle was inside for 30 s or 60 s, the fuel vaporized immediately after the jet and droplets hit the surface of the cell at 190°C and 290°C. Due to the high frequency of the camera, the whole vaporization time could not be captured. However, the evaporation duration is estimated to be between 3 and 5 s for hexane, Jet A, SPK, and 10% TMB. Furthermore, the injection of hexane was around 0.3s, but a big droplet dropped after 0.6 s, so there was an unsteady injection to be considered in the evaluation.

3.6 Background-Oriented Schlieren

The BOS technique measures displacements of the background image due to index of refraction changes caused to composition and density gradients. This enables the visualization of the fuel vapor dispersion and the flame propagation after ignition as both lead to a strong index of refraction variation. Processed images highlighting the process of vaporization for the four tested fuels are given in Figure 21 (33ms after the start of the injection), Figure 22 (67ms after the start of the injection), and Figure 23 (100ms after the injection). The colors of the images are scaled to be proportional to magnitude of the displacement gradients, where dark blue represents a low gradient (i.e. no fuel vapor), and yellow a high gradient (i.e high fuel vapor concentration or liquid phase). From Table 10, the hexane injection is the slowest, which is also visible in the BOS images. In other tests (Figure 26), we observed that hexane is visible with the BOS settings we used, and infer that slow injection must be the cause of the low detection of the vapor flow compared to the other fuels. Apparently, slow injection reduces the gradients in composition and density during vapor dispersion. Otherwise, the vapor dispersion pattern appears consistent across all fuels, indicating that fluid dynamics predominantly govern the flow, with minimal impact from the fuel characteristics.

A vertical profile of image intensity (converted to a grey scale) has been made from a 3-pixel wide area on the right side of the images with the intention of characterizing the impact of the small differences in fuel characteristics of Jet A, SPK, and 10% TMB, and to illustrate the dissimilarity to hexane on the vapor flow. Results are shown in Figure 24, where the greyscale values of the pixels positioned over the red line, which is added to the color version image, are plotted on graphs and investigated over time. The vertical position in the cell is given in pixels, where 680 represents the bottom of the cell and 0 the top. The same observations as in the processed BOS images can be made. Over time, the flow dispersed towards the top of the cell for all fuels except for hexane since the gradient is too small to be detected by the BOS technique. It is likely that the grey scale profiles do not deliver more information since the processed data are noisy and the border of the vapor cloud is difficult to extract numerically.

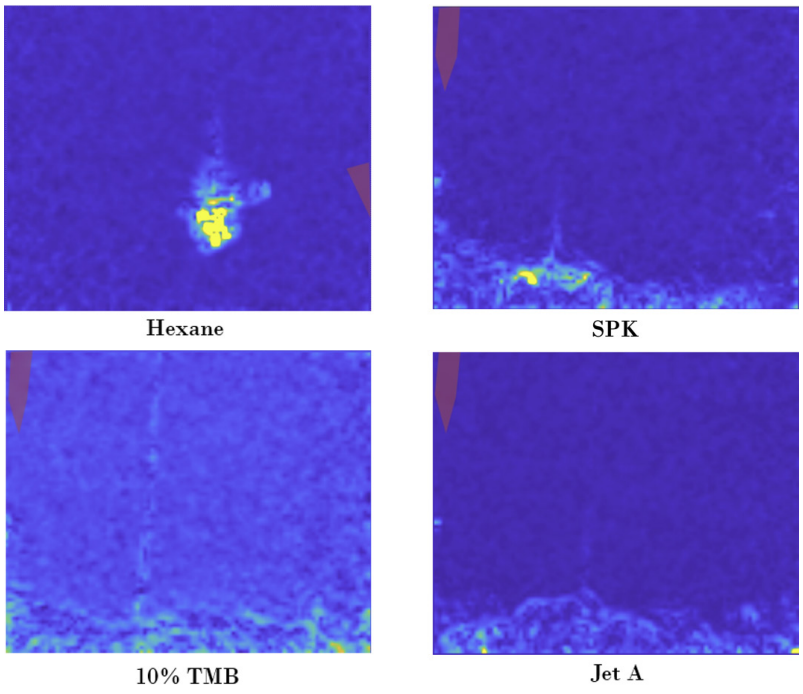

Figure 21: BOS images to visualize vaporization of different fuels 33 ms after injection start

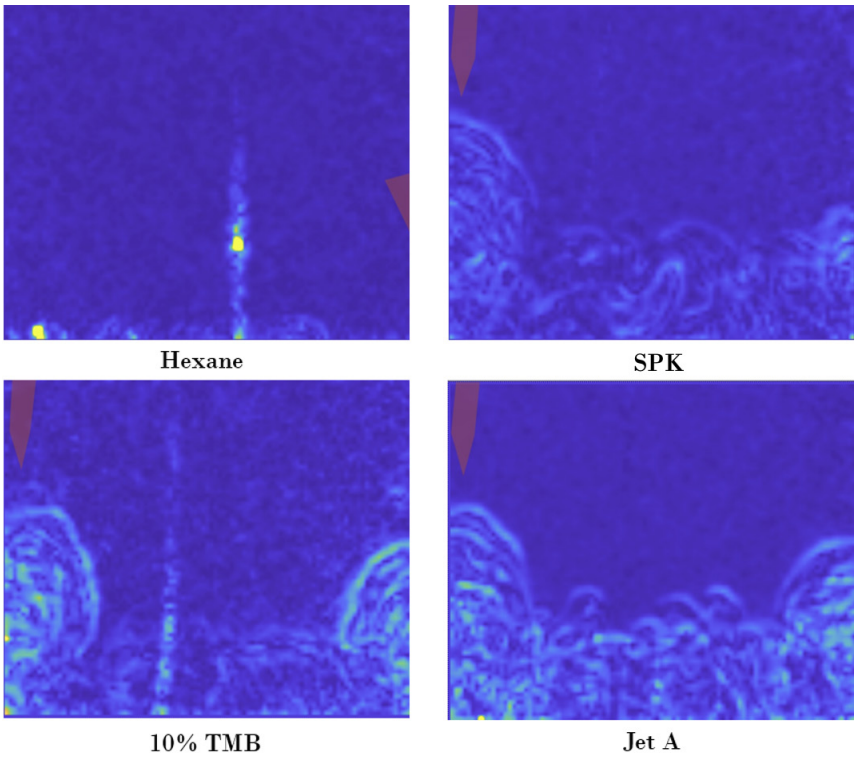

Figure 22: BOS images to visualize vaporization of different fuels 67 ms after injection start

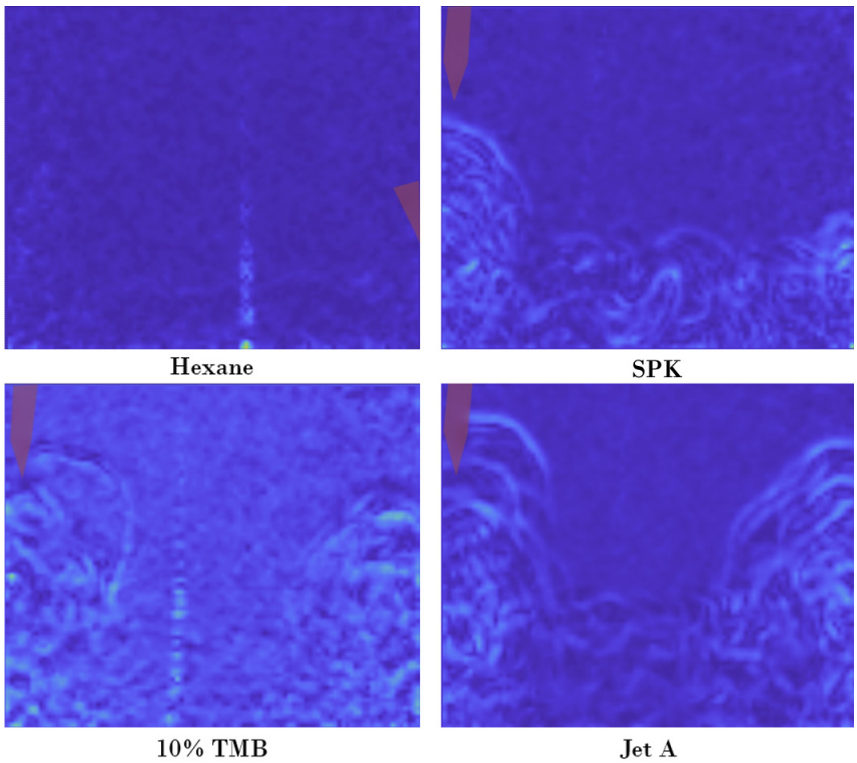

Figure 23: BOS images to visualize vaporization of different fuels 100 ms after injection start

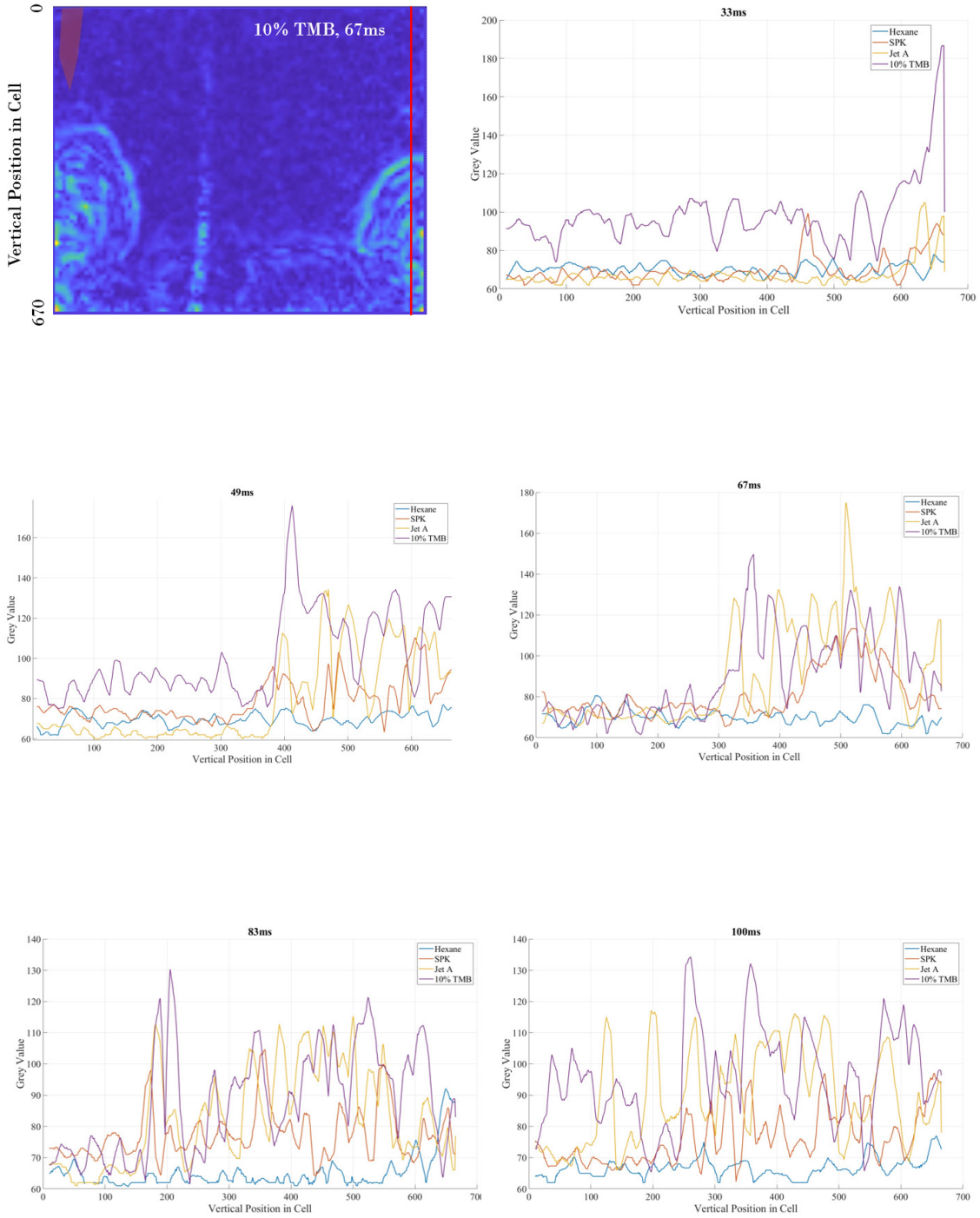

Figure 24: Image intensity profile of vapor dispersion of area marked with red line over time for hexane, SPK, Jet A and 10% TMB

While the images suggest that vapor only rises along the side walls, this is an artifact of the setup. In reality, the vapor expands radially outward and then upward within the 3-dimensional cell. When viewed from the front, the camera records a thicker vapor volume and gradient near the walls, creating the impression that the flow is concentrated there, as visually explained in Figure 25.

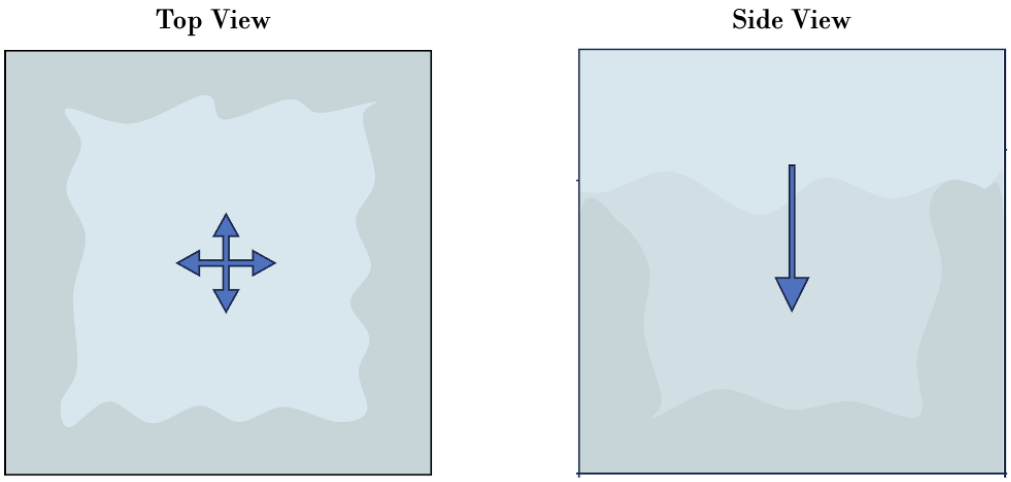

Figure 25: Explanation for appearance of processed BOS images

We also confirmed the occurrence of unintentional injection when the needle overheats inside the flask. Figure 26 validates the hypothesis that if the needle remains too long in the hot-air atmosphere, fuel is prematurely released into the flask, increasing the internal fuel volume by up to 150%. This test, conducted at 290°C with hexane, showed that after the needle was inside the cell for 3-5 seconds, 50 µL of the 100 µL hexane in the needle was injected without operating the syringe. To prevent this in the future, the needle should be filled with air after loading the syringe with fuel, ensuring that any fuel in the needle is not released into the flask before the intended injection.

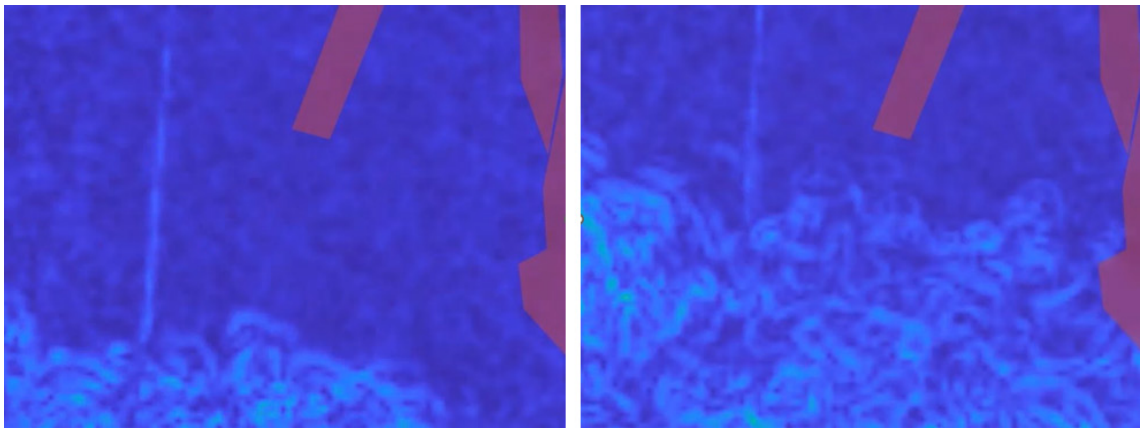

Figure 26: Validation for unintentional injection in hot atmosphere

With the BOS technique, it is also possible to observe the flame propagation in the cell. Comparing the following four figures, it is clear that all four tests have an ignition kernel on top of the cell. For the test with hexane (Figure 27), a first weak flame is visible, followed by the hot flame. We believe that the first ignition is a cold flame, which can be validated using a spectrometer or color camera in the future. For the tests with SPK and Jet A (Figure 28 and 29), propagation along the walls occurs, whereas with 10% TMB (Figure 30), we observed two ignition kernels, one at the top and one at the bottom.

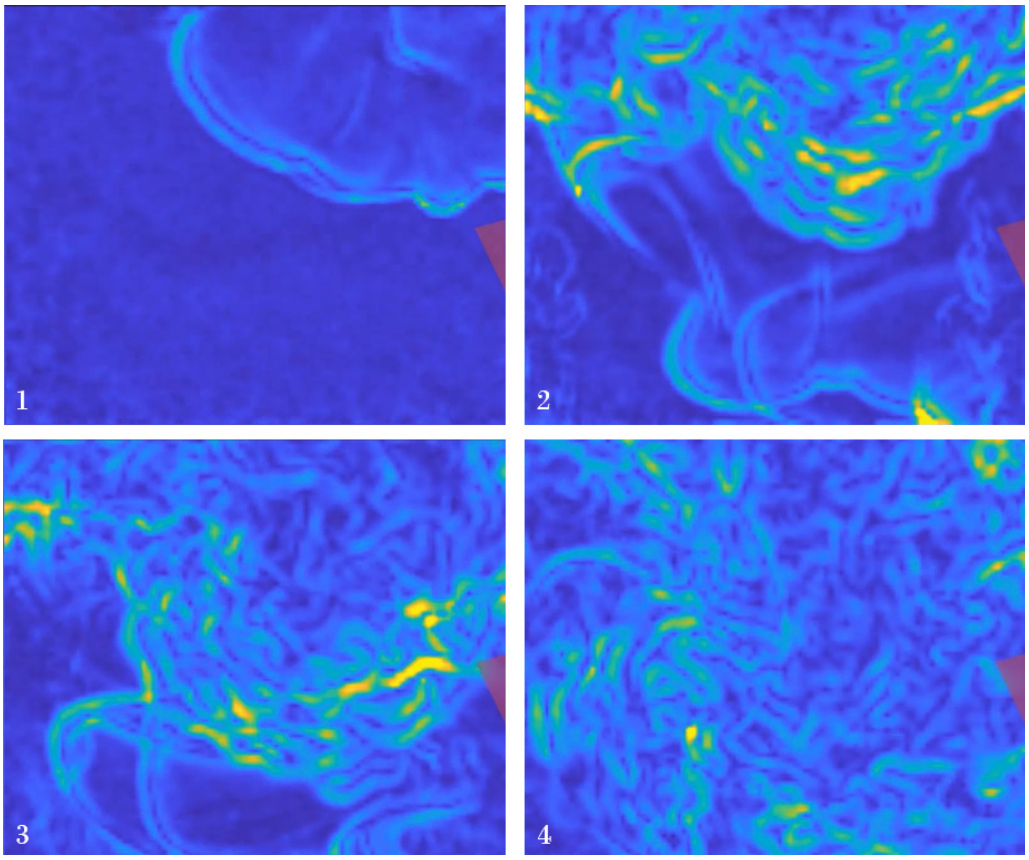

Figure 27: Visualization of the flame propagation with hexane

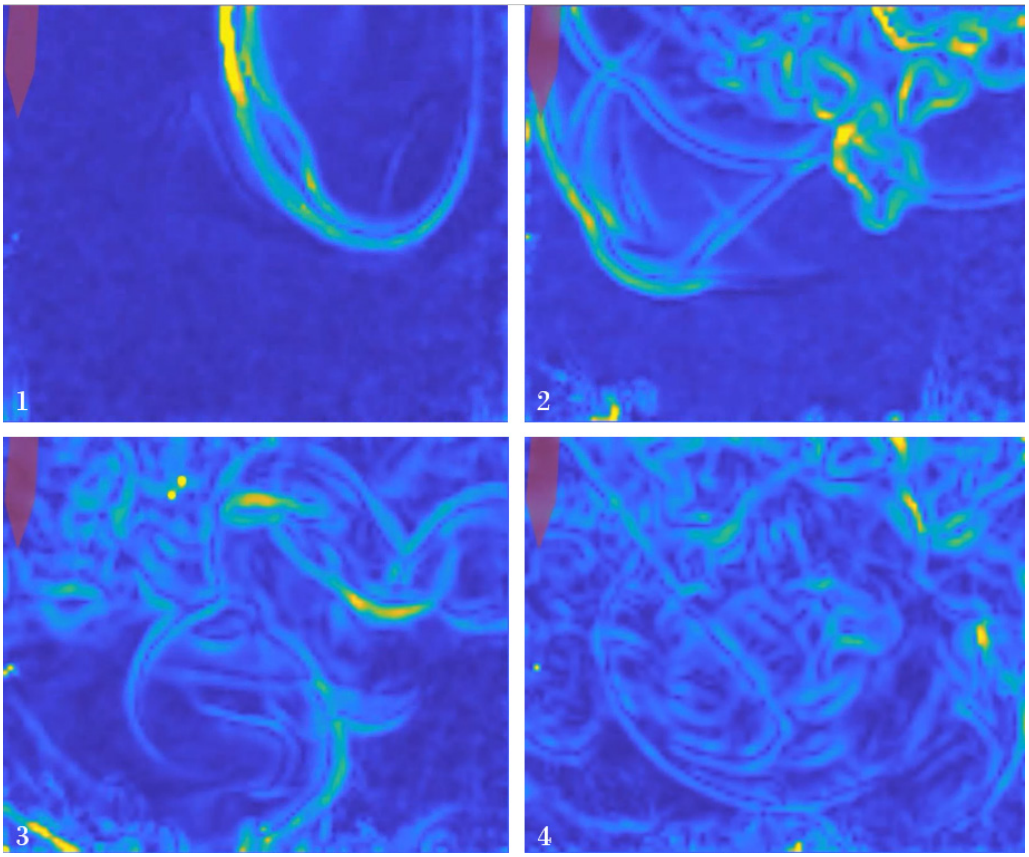

Figure 28: Visualization of the flame propagation with SPK

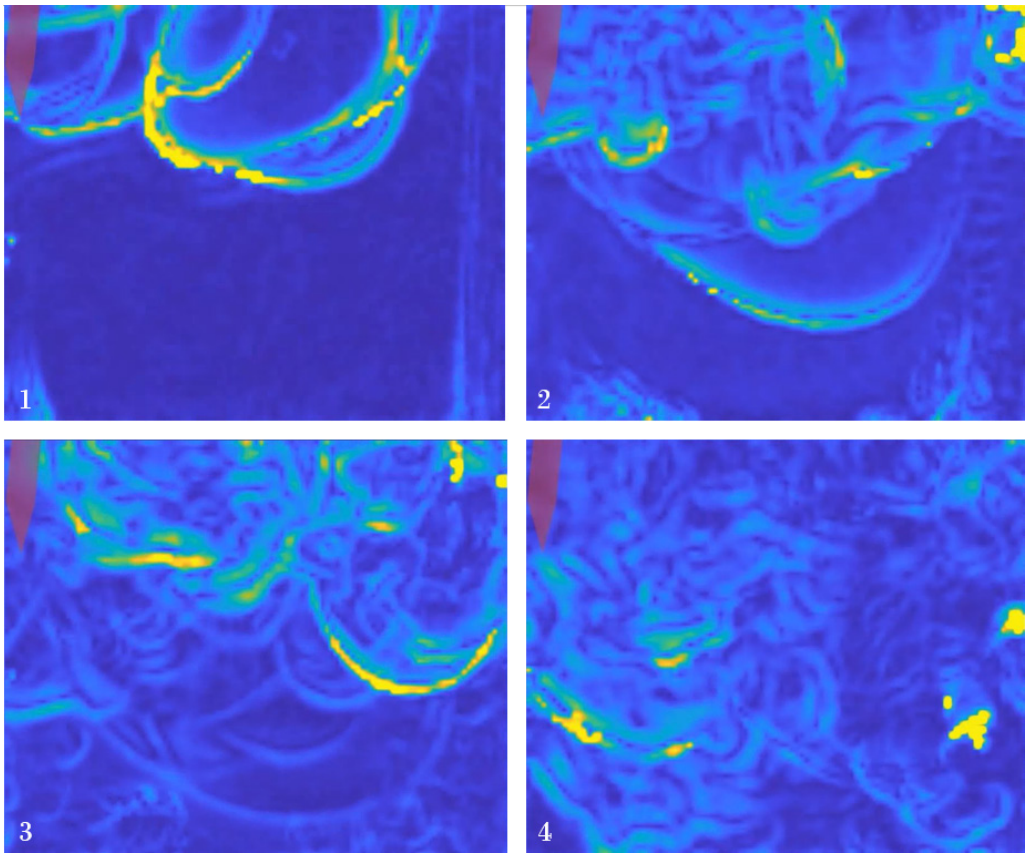

Figure 29: Visualization of the flame propagation with Jet A

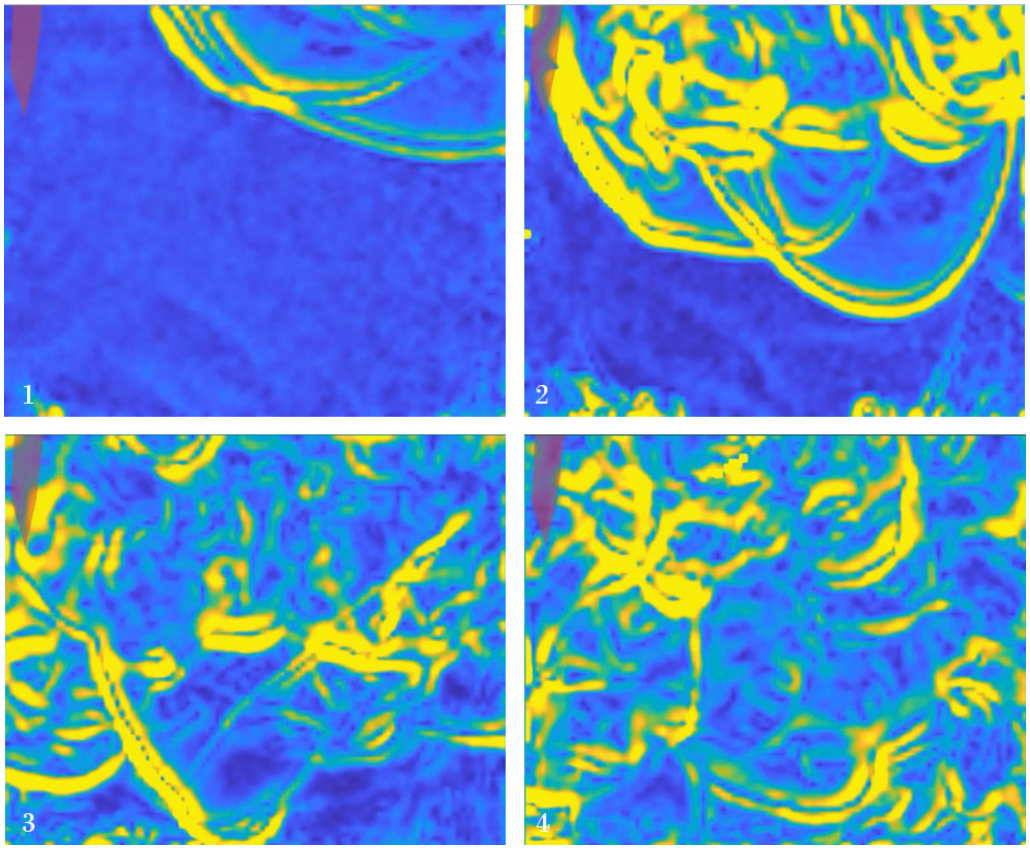

Figure 30: Visualization of the flame propagation with 10% TMB

3.7 Comparison Between Injection of Liquid and Gaseous Hexane

Given that flow visualization revealed the unintentional injection of fuel produces a multiphase vapor jet, the impact of this gaseous state on ignition behavior was further investigated by using the ASTM-E659 test to inject gaseous hexane. Due to a bigger syringe, which is incompatible with the automated injection system, the injection was made manually. The results are meant to be preliminary to give an initial idea of whether the aggregate state greatly affects the ignition behavior.

The syringe was filled with 0.1 mL - 0.4 mL of liquid hexane and 50 mL or 150 mL of air. Because of the relatively high vapor pressure of hexane, it vaporizes in the syringe while speeding the process up by putting the syringe under hot water. The volume of liquid hexane expands by a factor of 200 when it vaporizes. When there was no liquid visible, the gaseous hexane-air mixture was manually injected into the flask at a temperature of 234°C - 242°C. The testing results are shown in Figure 31. During the testing series at 239°C - 241°C, Mode I and III ignitions were observed. This shows that the gaseous hexane ignition is possible inside the ASTM flask. Tests at lower temperatures have also been conducted without ignition. The increase of 5°C to achieve a Mode I ignition must be acknowledged without knowing yet if it is due to the vapor phase or the injection conditions. Continuing the investigation and improving the injection of gaseous hexane ignition will deliver more reliable results.

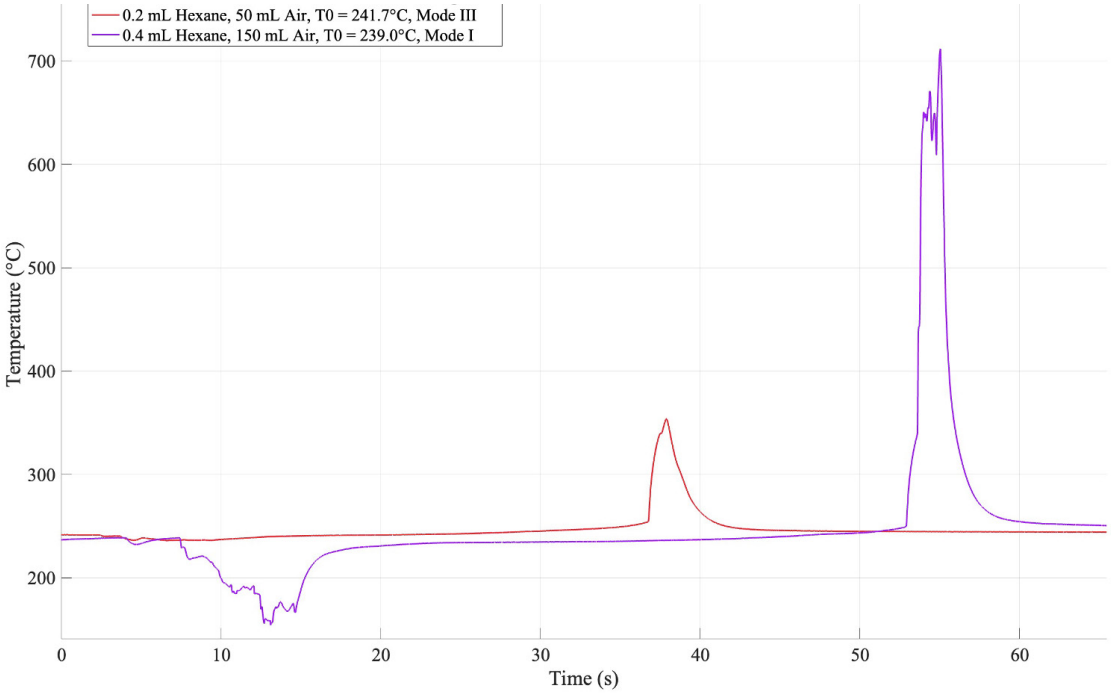

Figure 31: Time-temperature plot for the ASTM-E659 tests with gaseous hexane

4 Conclusions and Future Work

The ASTM-E659 testing method is the standard for evaluating fuel autoignition hazards due to fuel-air mixtures adjacent to hot surfaces. However, the test protocol lacks specificity, particularly regarding injection parameters, potentially leading to variability in test results across different laboratories. To enhance the reliability of this test, it is crucial to understand how the test setup influences the ignition behavior of fuels. This project investigated the impact of injection parameters on ignition behavior during the ASTM-E659 test using an automated injection system developed by the Explosion Dynamics Laboratory.

After proving the repeatability of the injection, the first focus was on the influence of the injection speed, the duration of the needle staying inside the flask before and after the injection, and the ignition delay time. The results indicated that varying the injection speed did not significantly affect ignition delay time. However, if the needle remains inside the flask longer before injection, ignition occurs faster, whereas ignition is delayed if it stays inside longer after injection. Analyzing the temperature signal plots revealed variability in the initial temperature drop, prompting a deeper investigation into this phenomenon.

A test conducted without fuel injection confirmed that the substantial temperature drop observed after injection was not caused by the insertion of the cold needle into the hot flask, as previously thought, but rather by the vaporization of the fuel. The temperature drop of approximately 10 K would typically cool 3.3 L of air. Yet, the flask only contains 500 mL, indicating that the heat transfer from the flask walls reduces the temperature drop, and the cooling during vaporization is not adiabatic.

The analysis of the temperature signal during vaporization showed that if the needle remains inside the flask for more than 9 seconds at the AIT, an unintentional hexane injection occurs, leading to a second vaporization event that increases the fuel volume by up to 150%. A hissing noise can be heard when this phenomenon happens. Using a new experimental cell setup, the injection jet was visualized, capturing this unintentional injection as a multiphase vapor jet. Flow visualization revealed that ignition occurs before the complete vaporization of all droplets. The BOS technique showed that while the mixing processes are consistent across different fuels, a slower injection rate appears to reduce the magnitude of the gradients.

Conducting ASTM-E659 tests with gaseous hexane showed that the ignition of gaseous hexane is possible at temperatures comparable to those of liquid fuel autoignition. However, since the gas injection method was improvised, further refinement is needed to quantify the differences in ignition behavior between liquid and gas phase injection. This would also allow a better understanding of the unintentional multiphase vapor injection in the ASTM-E659 test.

A future goal would be to visualize the processes within ASTM-E695 so that the injection jet, ignition behavior, and flame propagation can be analyzed as a function of test parameters.

Acknowledgements

I sincerely thank Dr. Joseph Shepherd for the opportunity to conduct research as an undergraduate in the Explosion Dynamics Laboratory this summer. I also wish to extend my thanks to Dr. Charline Fouchier for her invaluable guidance and expertise throughout the project. This experience would not have been possible without the support of The Boeing Company and the generous contribution from the Toshi Kubota Aeronautics SURF Fellow donors.

References

[1] ASTM International. ASTM E659-15, Standard Test Method for Autoignition Temperature of Liquid Chemicals. Standard, 2015.

[2] Conor D Martin and Joseph E Shepherd. Low temperature autoignition of jet a and surrogate jet fuel. *Journal of Loss Prevention in the Process Industries*, 71:104454, 2021.

[3] Frédérique Battin-Leclerc. Detailed chemical kinetic models for the low-temperature combustion of hydrocarbons with application to gasoline and diesel fuel surrogates. *Progress in Energy and Combustion Science*, 34(4):440–498, 2008.

[4] Charline Fouchier and Joseph Shepherd. ASTM E659 standardized test analysis and results for synthetic paraffinic kerosene. *15th International Symposium on Hazards, Prevention and Mitigation of Industrial Explosions*, 2024.

[5] Conor Daniel Martin. *Experiments in Thermal Ignition: Influence of Natural Convection on Properties of Gaseous Explosions*. PhD thesis, California Institute of Technology, 2023.

[6] Jearl Walker. Boiling and the leidenfrost effect. *Fundamentals of physics*, pages E10–1, 2010.

[7] R Mével, F Rostand, D Lemarié, L Breyton, and JE Shepherd. Oxidation of n-hexane in the vicinity of the auto-ignition temperature. *Fuel*, 236:373–381, 2019.

[8] TM Aminabhavi, VB Patil, MI Aralaguppi, and HTS Phayde. Density, viscosity, and refractive index of the binary mixtures of cyclohexane with hexane, heptane, octane, nonane, and decane at (298.15, 303.15, and 308.15) K. *Journal of Chemical & Engineering Data*, 41(3):521–525, 1996.

[9] Vladimír Majer, Václav Svoboda, Slavoj Hála, and Jiří Pick. Temperature dependence of heats of vaporization of saturated hydrocarbons C5-C8; experimental data and an estimation method. *Collection of Czechoslovak Chemical Communications*, 44(3):637–651, 1979.

[10] The Engineering ToolBox. Air - specific heat vs. pressure at constant temperature. `https://www.engineeringtoolbox.com/air-specific-heat-various-pressures-d_1535.html`, 2009. Accessed: 8/15/2024.